MRI Signal Reconstruction via Fourier Frames on Interleaving Spirals
Project Proposal

Christiana Sabett
Applied Mathematics, Applied Statistics, & Scientific Computation

Advisors: John Benedetto, Alfredo Nava-Tudela
Mathematics, IPST

October 15, 2015

1 Abstract

This project aims to effectively reconstruct an MRI signal using Fourier frames. We begin by describing the theoretical framework of a Fourier frame on the Paley-Wiener space $PW_{\overline{B(0,R)}}$. We then invoke Beurling's theorem to prove that we can choose points along interleaving spirals in the spectral domain to construct a Fourier frame for $PW_{\overline{B(0,R)}}$. We use frame notation to extend these results to the signal space of a square image, forming a reconstruction algorithm that results in an overdetermined linear system. We implement two different algorithms to solve the least-squares approximation in order to recover the spatial components of the MRI signal.

2 Background

MRI signal reconstruction from spectral sampling is a common problem in the field of signal processing. Formally stated, image reconstruction is an inversion problem: given frequency information, we want to recover the spatial components of the image. MRI reconstruction in particular desires both speed and accuracy, but often the former is neglected. Previous results have shown that sampling on interleaving spirals in the spectral domain makes for much faster data acquisition than rectilinear spectral sampling [7, 5]. We desire a reconstruction scheme that makes use of this data acquisition method. The standard approach to MRI reconstruction relies on uniform sampling of the spectral domain [10]. We will show that by sampling nonuniformly along the interleaving spirals, we can construct a Fourier frame approximant that allows us to achieve perfect MRI reconstruction.

It is well-established that uniform sampling in the spectral domain of a band-limited signal can produce perfect reconstruction (Shannon's theorem), i.e. the reconstructed signal is a scaled, delayed version of the original signal. This result leads to the Nyquist sampling theorem, which states that to obtain perfect reconstruction, a band-limited signal must be sampled at a rate at least twice the maximum frequency [10]. Rectilinear sampling in the spectral domain consists of points (λ, μ) where $\lambda = mh_\lambda$ and $\mu = nh_\mu$ for $m, n \in \mathbb{Z}$ and for fixed distances between coordinates h_λ and h_μ that satisfy the Nyquist criterion. The typical MRI reconstruction algorithm samples rectilinearly and then applies the Fast Fourier Transform to recover the image [6, 10].

A standard MRI machine measures the exact spectral components of the signal. Coils generate a magnetic field that causes the body's protons to align with it along a magnetic vector. A radio wave frequency (RF) is then passed through the body to disrupt the magnetic field, forcing the protons out of equilibrium. Once the pulse passes, the protons realign with the magnetic field. The time it takes for the particles to return

to homeostasis and the amount of energy released indicate the type of tissue the pulses are moving through. Localizing the magnetic field allows for the recovery of images such as Figure 1 [4, 11].

Figure 1: "Carolyn's MRI", by ClintJCL (Flickr)

3 Theoretical Approach

The *Paley-Wiener space* PW_E is defined as

$$PW_E = \{\varphi \in L^2(\widehat{\mathbb{R}}^d) : \text{supp } \varphi^\vee \subseteq E\},$$

where $\widehat{\mathbb{R}}^d$ is the domain of the Fourier transforms of signals in d-dimensional Euclidean space, and $L^2(\widehat{\mathbb{R}}^d)$ is the space of finite energy signals on $\widehat{\mathbb{R}}^d$ with $E \subseteq \mathbb{R}^d$ compact. The Fourier transform of a signal $f(x)$ is defined as $\mathcal{F} : L^2(\mathbb{R}^d) \to L^2(\widehat{\mathbb{R}}^d)$ such that $\mathcal{F}(f)(\omega) = \int_{-\infty}^{\infty} f(x)e^{-2\pi i x\cdot\omega}dx$. $\varphi^\vee$ denotes the inverse Fourier transform of φ and supp $\varphi^\vee$ denotes the support of $\varphi^\vee$ [3].

In a separable Hilbert space H, a *frame* is defined as a sequence $\{x_n : n \in \mathbb{Z}^d\} \subseteq H$ for which there exist $A, B > 0$ such that

$$\forall y \in H, \quad A||y||^2 \leq \sum_n |\langle y, x_n\rangle|^2 \leq B||y||^2.$$

Let $\Lambda \subseteq \widehat{\mathbb{R}}^d$ be a sequence and let $E \subseteq \mathbb{R}^d$ be compact. Define the sequence $\{e_\lambda \mathbb{1}_E : \lambda \in \Lambda\} \subseteq L^2(\mathbb{R}^d)$, where $e_\lambda(x) = e^{-2\pi i x\cdot\lambda}$. In particular, note that $(e_\lambda \mathbb{1}_E)^\wedge \in PW_E$ and $L^2(E) = (PW_E)^\vee$. The sequence $\{e_\lambda \mathbb{1}_E\}$ is a frame for $L^2(E)$ (where we write $L^2(E) \subseteq L^2(\mathbb{R}^d)$ because $(PW_E)^\vee \subseteq L^2(\mathbb{R}^d)$), if and only if there exist $0 < A \leq B < \infty$ such that

$$\forall f \in L^2(E), \quad A||f||^2_{L^2(E)} \leq \sum_{\lambda\in\Lambda} |\langle f, e_\lambda \mathbb{1}_E\rangle_{L^2(E)}|^2 \leq B||f||^2_{L^2(E)}$$

where $\langle f, e_\lambda \mathbb{1}_E\rangle_{L^2(E)} = \int_E f(x)e^{-2\pi i x\cdot\lambda}dx = \widehat{f}(\lambda)$. We can further say that the sequence $(e_\lambda \mathbb{1}_E)^\wedge$ is a frame for PW_E if $\{e_\lambda \mathbb{1}_E\}$ is a frame for $L^2(E)$. We call such a sequence a *Fourier frame for* PW_E [1, 3].

A set Λ is *uniformly discrete* if there exists $r > 0$ such that

$$\forall \lambda, \gamma \in \Lambda, \quad |\lambda - \gamma| \geq r.$$

When E is the closed ball $\overline{B(0,R)} \subset \mathbb{R}^d$ centered at $\mathbf{0}$ with radius R, Beurling's theorem tells us the following [3]: Let $\Lambda \subseteq \widehat{\mathbb{R}}^d$ be uniformly discrete and let $\text{dist}(\xi, \Lambda) = \inf_{\lambda \in \Lambda} \sqrt{\sum_{i=1}^d |\xi_i - \lambda_i|^2}$ denote the Euclidean distance between the point ξ and the set Λ. Define

$$\rho = \rho(\Lambda) = \sup_{\xi \in \widehat{\mathbb{R}}^d} \text{dist}(\xi, \Lambda).$$

If $R\rho < \frac{1}{4}$, then Λ is a Fourier frame for $PW_{\overline{B(0,R)}} \subseteq L^2(\widehat{\mathbb{R}}^d)$.

Define $L : L^2(E) \to \ell^2(\Lambda)$ of a Bessel map such that $f \to \{\widehat{f}(\lambda) : \lambda \in \Lambda\}$. Let L^* be its adjoint, and define the frame operator

$$S = L^*L : L^2(E) \to L^2(E)$$

such that $f \to S(f) = \sum_{\lambda \in \Lambda} \widehat{f}(\lambda) e_\lambda \mathbb{1}_E$. If $\{e_\lambda \mathbb{1}_E\}$ is a frame for $L^2(E)$, then

$$f = SS^{-1}f = \sum_{\lambda \in \Lambda} (S^{-1}f)^\wedge(\lambda) e_\lambda \mathbb{1}_E. \tag{1}$$

From this we can conclude that every finite energy signal $f \in L^2(E)$ can be represented as

$$f(x) = \sum_{\lambda \in \Lambda} a_\lambda(f) e_\lambda \mathbb{1}_E \tag{2}$$

in $L^2(\mathbb{R}^d)$, where $a_\lambda(f) = (S^{-1}f)^\wedge(\lambda)$ and $\sum_{\lambda \in \Lambda} |a_\lambda(f)|^2$ is finite.

Given the representation in (2), we must now choose a sequence $\Lambda_R \in \widehat{\mathbb{R}}^d$ such that Λ_R is a Fourier frame for $PW_{\overline{B(0,R)}}$. Let $c, R > 0$, and let $\{A_k : k = 0, 1, ..., M-1\}$ denote a finite set of interleaving Archimedean spirals of the form

$$A_k = \{c\theta e^{2\pi i(\theta - (k/M))} : \theta \geq 0\}.$$

Let $B = \cup_{k=1}^{M-1} A_k$. We will construct a uniformly discrete set $\Lambda_R \subseteq B$ that will form a Fourier frame for $PW_{\overline{B(0,R)}}$.

First, choose M such that $\frac{cR}{M} < 1/2$. For any given $\xi_0 \in \widehat{\mathbb{R}}^2$, we will write it as $\xi_0 = r_0 e^{2\pi i \theta_0}$ where $r_0 \geq 0$ and $\theta_0 \in [0, 1)$. Then either $0 \leq r_0 < c\theta_0 < c$ or there exists $n_0 \in \mathbb{N} \cup \{0\}$ for which

$$c(n_0 + \theta_0) \leq r_0 < c(n_0 + 1 + \theta_0).$$

In the second case, we can find $k \in \{0, \cdots, M-1\}$ such that

$$c(n_0 + \theta_0 + \frac{k}{M}) \leq r_0 < c(n_0 + \theta_0 + \frac{k+1}{M}),$$

which implies

$$\text{dist}(\xi_0, B) \leq \frac{c}{2M}.$$

Next, choose $\delta > 0$ such that $R\rho < 1/4$, where $\rho = (c/2M) + \delta$. For each k, we choose a uniformly discrete set of points Λ_k along the spiral A_k, where the curve distance between consecutive points is less than 2δ, beginning within 2δ of the origin. This rule guarantees that the distance from any point on the spiral A_k to Λ_k is less than δ. Finally, set $\Lambda_R = \cup_{k=0}^{M-1} \Lambda_k$. By the triangle inequality,

$$\begin{aligned} \forall \xi \in \widehat{\mathbb{R}}^2, \quad \text{dist}(\xi, \Lambda_R) &\leq \text{dist}(\xi, B) + \text{dist}(B, \Lambda_R) \\ &\leq \frac{c}{2M} + \delta = \rho. \end{aligned}$$

Recall that by our choices of δ and M, we have that $R\rho < 1/4$, thus Beurling's theorem tells us Λ_R is a Fourier frame for $PW_{\overline{B(0,R)}}$.

4 Problem Construction

We shall extend the results in Section 3 to the signal space of a square image of size $N \times N$ in $\mathbb{R}^2$ [3]. Consider the image $f \in L^2([-\frac{1}{2}, \frac{1}{2}]^2)$, taken to be zero outside of $[-\frac{1}{2}, \frac{1}{2}]^2$. We assume that f is piecewise constant. We then partition the image into subsquares of size $\frac{1}{N} \times \frac{1}{N}$, closed on the left and upper edges. To illustrate: in any subsquare, we have point $p = (x, y) \in (-\frac{1}{2}, \frac{1}{2}) + [\frac{m}{N}, \frac{m+1}{N}) \times [\frac{n}{N}, \frac{n+1}{N})$ where $m, n = 0, 1, ..., N-1$. Then let $f_{m,n} \in \mathbb{R}$ be the value of f in the (m, n) subsquare. Thus, we can simply write f as a sum of the characteristic functions of each subsquare, such that

$$f(p) = \sum_{m,n=0}^{N-1} f_{m,n} \mathbb{1}_{\square_{m,n}}(p), \tag{3}$$

where $\square_{m,n}$ denotes the subsquare $(-\frac{1}{2}, \frac{1}{2}) + [\frac{m}{N}, \frac{m+1}{N}) \times [\frac{n}{N}, \frac{n+1}{N})$. Since f is piecewise constant, we can consider sampling along each dimension separately, so (3) becomes

$$f(x, y) = \sum_{m,n=0}^{N-1} f_{m,n} \mathbb{1}_{[\frac{m}{N}, \frac{m+1}{N})}(x) \mathbb{1}_{[\frac{n}{N}, \frac{n+1}{N})}(y). \tag{4}$$

Recall that the MRI machine samples the Fourier transform in $\widehat{\mathbb{R}}^2$. We therefore examine the signal in the spectral domain. Taking the Fourier transform of $f(x, y)$ gives

$$\widehat{f}(\lambda, \mu) = \sum_{m,n=0}^{N-1} f_{m,n} \widehat{\mathbb{1}}_{[\frac{m}{N}, \frac{m+1}{N})}(\lambda) \widehat{\mathbb{1}}_{[\frac{n}{N}, \frac{n+1}{N})}(\mu). \tag{5}$$

Let $H_{m,n}(\alpha) = H_{m,n}(\lambda, \mu) = \widehat{\mathbb{1}}_{[\frac{m}{N}, \frac{m+1}{N})}(\lambda) \widehat{\mathbb{1}}_{[\frac{n}{N}, \frac{n+1}{N})}(\mu)$ for convenience. Then (5) becomes

$$\widehat{f}(\alpha) = \sum_{m,n=0}^{N-1} f_{m,n} H_{m,n}(\alpha) \tag{6}$$

We restrict our view of the spectral domain to the square $[-\frac{K}{2}, \frac{K}{2})^2$. The choice of K will be (experimentally) determined based on a desired error threshold. From our earlier result (2), we need a sequence of points to construct a Fourier frame for our space. Within this restricted domain, we choose $M \geq N^2$ points $\alpha_i = (\lambda_i, \mu_i)$ for $i = 0, 1, ..., M-1$ on the interleaving spirals such that the α_i are nonuniform in the square. Let $\Lambda = \{\alpha_i\}$. We extend this tiling to the entire spectral domain by utilizing the periodic extension $\Lambda + K\mathbb{Z}^2$, creating a frame $\mathcal{F}$ for PW_E, where $E = [-\frac{1}{2}, \frac{1}{2}]^2$.

For convenience, we define a lexicographical ordering of the grid points $b_j = (m_j, n_j)$ such that $j = 0, 1, ..., N^2 - 1$. From (6), we now have

$$\widehat{f}(\alpha_i) = \sum_{j=0}^{N^2-1} f_{b_j} H_{b_j}(\alpha_i). \tag{7}$$

Let

$$\widehat{\mathbb{F}} = [\widehat{f}(\alpha_0)\ \widehat{f}(\alpha_1)\ ...\ \widehat{f}(\alpha_{M-1})]^{\mathrm{T}}$$

and

$$\mathbb{F} = [f_{b_0}\ f_{b_1}\ ...\ f_{b_{N^2-1}}]^{\mathrm{T}}.$$

Define $\mathbb{H}$ such that $\mathbb{H} = [H_{b_j}(\alpha_i)]_{i,j}$, and (7) becomes

$$\widehat{\mathbb{F}} = \mathbb{H}\mathbb{F}. \tag{8}$$

The matrix equation (8) contains $M \geq N^2$ points in the spectral domain and N^2 points in the spatial domain. $\widehat{\mathbb{F}}$ is a length-M vector, $\mathbb{F}$ is a length-N^2 vector, and $\mathbb{H}$ is size $M \times N^2$. This yields an overdetermined system. $\mathbb{F}$ contains the spatial components of the image f that we wish to recover. In the following section, we will show that this matrix representation is equivalent to the frame reconstruction scheme.

5 Problem

The goal of this project is to use nonuniform sampling on interleaving spirals to define a Fourier frame in $\widehat{\mathbb{R}}^d$, from which we can reconstruct a low-resolution MRI image. We do not have access to real MRI data, so we will create a synthetic data set using high-resolution images.

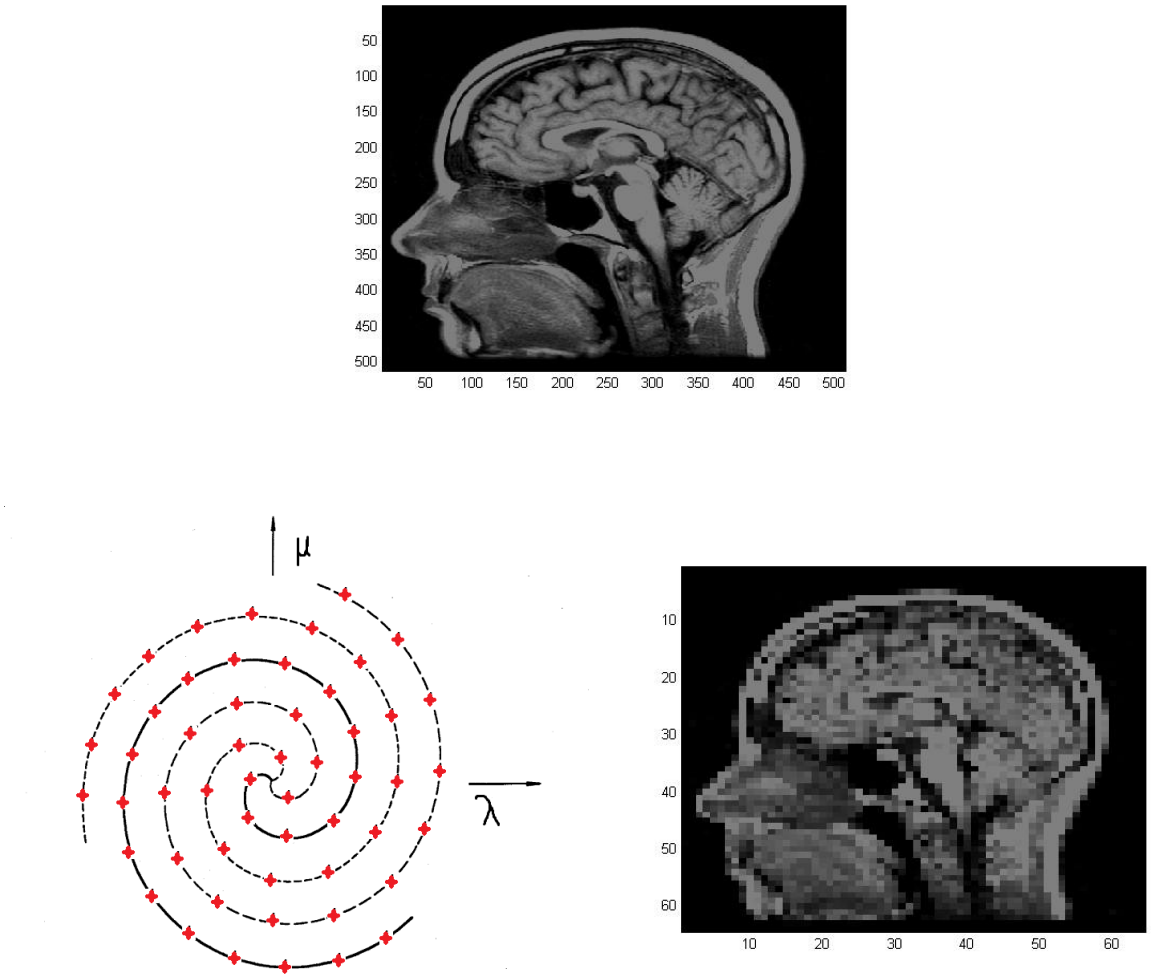

Figure 2: Problem overview. Top: High-resolution image f from which synthetic data is formed. Bottom left: Sampling along interleaving spirals in the spectral domain of the high-resolution image. Bottom right: Downsampled version of the high-resolution image that serves as the ideal reconstruction.

Given a high resolution image f, generally of size 1024×1024, downsample f to form f_N, an $N \times N$ approximant where $N = 128$ or $N = 256$. The $N \times N$ approximant f_N is the optimal available image at that resolution. We take this as our ideal reconstruction, from which the error will be computed. From the original image, f, we take the DFT at the points b_j to get $\widehat{f}$ as defined in (6). From $\widehat{f}$, we sample $\widehat{f}(\alpha_i)$ for $i = 0, 1, ..., M-1$ (with $M \geq N^2$) on a union of Archimedean spirals within the square $\left[-\frac{K}{2}, \frac{K}{2}\right)^2$ (Figure 2).

Beurling's theorem allows us to develop a reconstruction scheme using the set of points $\Lambda = \widehat{f}(\alpha_i)$. The frame definition gives rise to a mapping $\mathbb{H}$ of N^2 points to M points, thus $\mathbb{H}$ is the matrix representation of the Bessel map $L : \ell^2(\{0, 1, ..., N^2 - 1\}) \to \ell^2(\{0, 1, ..., M - 1\})$, $\mathbb{H}^*$ is its adjoint L^*, and $\mathbb{H}^*\mathbb{H}$ is equivalent to the frame operator $S = L^*L$. The frame reconstruction scheme is

$$f = (S^{-1}L^*)Lf. \tag{9}$$

Setting $Lf = \widehat{f}$, our reconstructed image $\tilde{f}$ takes the form

$$\tilde{f} = S^{-1}L^*\widehat{f}. \tag{10}$$

Applying the construction in Section 4 yields the overdetermined system in (8). We can see that in our frame terminology, the least-squares approximation

$$\mathbb{F} = (\mathbb{H}^*\mathbb{H})^{-1}\mathbb{H}^*\widehat{\mathbb{F}}, \tag{11}$$

where $\mathbb{H}^* := \overline{\mathbb{H}}^{\mathrm{T}}$, is equivalent to (9).

From $\tilde{f}$, we will compare our reconstruction with the optimal available image f_N by analyzing $f_N - \tilde{f}$.

6 Approach

A typical MRI image f is of size $N^2 = 256 \times 256$. Our primary concern is solving (11) by constructing $\widehat{\mathbb{F}}$ and $\mathbb{H}$ as described Section 5. Assuming $(\mathbb{H}^*\mathbb{H})^{-1}$ exists, f can be reconstructed. Note that $\mathbb{H}^*\mathbb{H}$ is fixed, which cuts down on storage costs considerably.

We will consider two reconstruction algorithms that solve the system

$$\mathbb{H}^*\mathbb{H}\mathbb{F} = \mathbb{H}^*\widehat{\mathbb{F}}. \tag{12}$$

The first is transpose reduction, which is the direct approach but with efficient storage. The second algorithm is the conjugate gradient method.

6.1 Transpose Reduction

This algorithm computes $\mathbb{H}^*\mathbb{H}$ directly as a sum of vector products instead of inefficiently storing $\mathbb{H}$ and then computing $\mathbb{H}^*\mathbb{H}$ [3].

Define $V_k = (H_0(\alpha_k), ..., H_{N^2-1}(\alpha_k))^*$ such that

$$\mathbb{H} = \begin{pmatrix} H_0(\alpha_0) & \cdots & H_{N^2-1}(\alpha_0) \\ H_0(\alpha_1) & \cdots & H_{N^2-1}(\alpha_1) \\ \vdots & \vdots & \vdots \\ H_0(\alpha_{M-1}) & \cdots & H_{N^2-1}(\alpha_{M-1}) \end{pmatrix} = \begin{pmatrix} V_0^* \\ V_1^* \\ \vdots \\ V_{M-1}^* \end{pmatrix}.$$

Note that

$$\begin{aligned}
\mathbb{H}^*\mathbb{H} &= \begin{pmatrix} \sum_{k=0}^{M-1} \overline{H_0(\alpha_k)}H_0(\alpha_k) & \cdots & \sum_{k=0}^{M-1} \overline{H_0(\alpha_k)}H_{N^2-1}(\alpha_k) \\ & \vdots & \\ \sum_{k=0}^{M-1} \overline{H_{N^2-1}(\alpha_k)}H_0(\alpha_k) & \cdots & \sum_{k=0}^{M-1} \overline{H_{N^2-1}(\alpha_k)}H_{N^2-1}(\alpha_k) \end{pmatrix} \\
&= \sum_{k=0}^{M-1} \begin{pmatrix} \overline{H_0(\alpha_k)}H_0(\alpha_k) & \cdots & \overline{H_0(\alpha_k)}H_{N^2-1}(\alpha_k) \\ & \vdots & \\ \overline{H_{N^2-1}(\alpha_k)}H_0(\alpha_k) & \cdots & \overline{H_{N^2-1}(\alpha_k)}H_{N^2-1}(\alpha_k) \end{pmatrix} \\
&= \sum_{k=0}^{M-1} \begin{pmatrix} \overline{H_0(\alpha_k)} \\ \overline{H_1(\alpha_k)} \\ \vdots \\ \overline{H_{N^2-1}(\alpha_k)} \end{pmatrix} (H_0(\alpha_k)\ H_1(\alpha_k)\ \cdots\ H_{N^2-1}(\alpha_k)) \\
&= \sum_{k=0}^{M-1} V_k V_k^*.
\end{aligned}$$

Similarly,

$$\mathbb{H}^* \widehat{f} = \begin{pmatrix} \sum_{k=0}^{M-1} \overline{H_0(\alpha_k)} \widehat{f}_k \\ \vdots \\ \sum_{k=0}^{M-1} \overline{H_{N^2-1}(\alpha_k)} \widehat{f}_k \end{pmatrix} = \sum_{k=0}^{M-1} \widehat{f}_k V_k.$$

To construct $A = \mathbb{H}^*\mathbb{H}$ and $b = \mathbb{H}^* \widehat{f}$:

1. Set A to be the $N^2 \times N^2$ zero matrix.
2. For $k = 0 : M - 1$

   Set $V_k = (H_0(\alpha_k), ..., H_{N^2-1}(\alpha_k))^*$
   $A \leftarrow A + V_k V_k^*$
   $b \leftarrow b + \widehat{f}_k V_k$

From here, (12) can be solved directly using a QR or Cholesky decomposition. This method uses a factor of N^2/M less memory than the direct approach with naive storage. In testing, as we increase the value of M, we expect this savings to become more apparent.

6.2 Conjugate Gradient Algorithm

Given the construction of $\mathbb{H}^*\mathbb{H}$,

$$[\mathbb{H}^*\mathbb{H}f]_m = \sum_{j=0}^{N^2-1} f_j \sum_{k=0}^{M-1} \overline{H_m(\alpha_k) H_j(\alpha_k)},$$

where $[\mathbb{H}^*\mathbb{H}f]_m$ denotes the mth element of $\mathbb{H}^*\mathbb{H}f$. As in the Transpose Reduction algorithm, let $A = \mathbb{H}^*\mathbb{H}$ and $b = \mathbb{H}^* \widehat{f}$. Then, for symmetric, positive definite A, we apply the conjugate gradient method [8] to solve the system $Af = b$.

1. Choose f_0. Let $r_0 = b - Af_0$. Set $p_0 = r_0$.
2. for $n = 1$ until convergence

   $\gamma = (r_n^T r_n)/((Ap_n)^T p_n)$
   $f_{n+1} = f_n + \gamma p_n$
   $r_{n+1} = r_n - \gamma A p_n$
   if norm$(r_{n+1}) <$ tol, break
   $\beta_n = (r_{n+1}^T r_{n+1})/(r_n^T r_n)$
   $p_{n+1} = r_{n+1} + \beta_n p_n$

This algorithm generally has linear convergence, but the speed of convergence depends on the condition number of A. We will also develop a modified implementation of the conjugate gradient algorithm that uses only matrix-vector operations instead of explicitly storing the matrix A.

7 Validation

Validation will take the form of comparing our algorithms with already-established algorithms. Small problems (on the order of 64×64 pixels) can be solved directly. We can compare the results of the Transpose Reduction algorithm with the results of the direct solution using naive storage. For larger problems, the conjugate gradient algorithm should follow the same convergence trajectory as Matlab's version.

8 Testing

Testing will primarily consist of error analysis. It is important to note that frames are defined for a countably infinite number of points that span the entirety of the spectral domain. This could result in discrepancies when we try to recover the image using only a limited range of frequencies. One aspect of testing will be to explore how much frequency information we need to adequately recover f_N (i.e. how large our square $\left[-\frac{K}{2}, \frac{K}{2}\right)^2$ should be). We must also test how many points α_i we must sample (how large M should be relative to N^2). The final aspect of testing will be to analyze the condition number of $\mathbb{H}^*\mathbb{H}$ and how it affects the reconstruction.

We will use the peak signal-to-noise ratio (PSNR) and Structural Similarity index (SSIM) to measure the error between the ideal reconstruction and the recovered image.

8.1 PSNR

A standard measure of a reconstructed image is the peak signal-to-noise ratio (PSNR) [6]. It is defined in terms of the mean-squared error. Given our optimal available image f_N of $N \times N$ pixels and the reconstructed image $\tilde{f}$,

$$MSE = \frac{1}{N^2} \sum_{m=0}^{N-1} \sum_{n=0}^{N-1} (\tilde{f}(m,n) - f_N(m,n))^2$$

Then the PSNR, expressed in decibels (dB), is

$$PSNR = 10 \log \frac{max_{f_N}^2}{MSE} \tag{13}$$

where max_{f_N} is the maximum possible pixel value for f_N. As we anticipate using purely grayscale images for this project, $max_{f_N} = 255$.

8.2 SSIM

The structural similarity (SSIM) index is a measure of similarity between two images [9]. Let x and y be signals where one is assumed to be of perfect quality. The luminance of each image is estimated by the mean intensities μ_x and μ_y. The standard deviations σ_x and σ_y are used to estimate the signal contrast. The constants C_1 and C_2 are used as stabilizers for when $\mu_x^2 + \mu_y^2$ and $\sigma_x^2 + \sigma_y^2$ are close to zero. The final form of the SSIM index is

$$\text{SSIM}(x,y) = \frac{(2\mu_x\mu_y + C_1)(2\sigma_{xy} + C_2)}{(\mu_x^2 + \mu_y^2 + C_1)(\sigma_x^2 + \sigma_y^2 + C_2)}.$$

8.3 Platform

The project will be run in Matlab on an Acer Aspire V5 with 6GB of RAM.

9 Milestones

- Construct a Fourier frame via sampling on interleaving spirals.
- Implement the Transpose Reduction algorithm.
- Implement the conjugate gradient algorithm.

10 Timeline

- October 2015: Code the sampling routine to form the Fourier frame.
- November 2015: Proof of concept on small problems.

- December 2015: Code the transpose reduction algorithm and begin testing.
- January - February 2016: Code the conjugate gradient algorithm. Design and implement modified conjugate gradient algorithm.
- February - March 2016: Error analysis/testing. Explore how much frequency information we need to adequately recover f_N. Explore condition number of $\mathbb{H}^*\mathbb{H}$ and how it affects the reconstruction.
- April 2016: Finalize results.

11 Deliverables

- Synthetic data set
- Fourier frame sampling routine
- Transpose reduction routine
- Conjugate gradient routine
- Final report and error analysis

References

[1] Au-Yeung, Enrico, and John J. Benedetto. "Generalized Fourier Frames in Terms of Balayage." Journal of Fourier Analysis and Applications 21.3 (2014): 472-508.

[2] Benedetto, John J., and Hui C. Wu. "Nonuniform Sampling and Spiral MRI Reconstruction." Wavelet Applications in Signal and Image Processing VIII (2000).

[3] Benedetto, John J., Alfredo Nava-Tudela, Alex Powell, and Yang Wang. MRI Signal Reconstruction by Fourier Frames on Interleaving Spirals. Technical report. 2008.

[4] Berger, Abi. "Magnetic Resonance Imaging." BMJ : British Medical Journal. BMJ, 5 Jan. 2002. Web. 13 Oct. 2015.

[5] Bourgeois, Marc, Frank T. A. W. Wajer, Dirk Van Ormondt, and Danielle Graveron-Demilly. "Reconstruction of MRI Images from Non-Uniform Sampling and Its Application to Intrascan Motion Correction in Functional MRI." Modern Sampling Theory (2001): 343-63.

[6] I. Daubechies. *Ten Lectures on Wavelets*. Society for Industrial and Applied Mathematics, Philadelphia, PA, 1992.

[7] Mansfield, P. "Multi-planar Image Formation Using NMR Spin Echoes." J. Phys. C: Solid State Phys. Journal of Physics C: Solid State Physics 10.3 (1977).

[8] O'Leary, Dianne P. Scientific Computing with Case Studies. Philadelphia: Society for Industrial and Applied Mathematics, 2009.

[9] Wang, Z., A.C. Bovik, H.R. Sheikh, and E.P. Simoncelli. "Image Quality Assessment: From Error Visibility to Structural Similarity." IEEE Transactions on Image Processing IEEE Trans. on Image Process. 13.4 (2004): 600-12.

[10] Yan, Hong. Signal Processing for Magnetic Resonance Imaging and Spectroscopy. New York: Marcel Dekker, 2002.

[11] "Magnetic Resonance Imaging (MRI)." Magnetic Resonance Imaging (MRI). NIH. Web. 13 Oct. 2015.